Solid State Photochemical Reaction of *N*-(α,*β*-Unsaturated carbonyl)benzoylformamides

Masami Sakamoto,*,‡ Masaki Takahashi,† Tsutomu Fujita,† Shoji Watanabe,† Takehiko Nishio,† Ikuo Iida,† and Hiromu Aoyama§

Department of Applied Chemistry, Faculty of Engineering, Chiba University, Yayoi-cho, Inage-ku, Chiba 263, Japan, Department of Chemistry, The University of Tsukuba, Tsukuba, Ibaraki 305, Japan, and Department of Material Chemistry, Faculty of Textile Science and Technology, Shinshu University, Ueda, Nagano 386, Japan

Received March 18, 1997⊗

Photochemical reactions of various *N*-(α,*β*-unsaturated carbonyl)benzoylformamides both in solution and in a solid state were investigated. Under homogeneous conditions, all acyclic imides underwent photochemical 2 + 2 cycloaddition that resulted in the production of bicyclic oxetanes. *N*-Isopropyl- and *N*-benzyl-*N*-tigloylbenzoylformamides crystallized in a chiral space group, and the photolysis in the solid state yielded corresponding optically-active oxetanes. *N*-Tigloylbenzoylformanilide underwent cis−trans isomerization to yield a photostationary state (cis/trans = 1.3). Solid state oxetane formation of *N*-benzyl- and *N*-(*o*-tolyl)- and *N*-(2,6-xylyl)-*N*-tigloylbenzoylformamides progressed via the crystal-to-crystal pathway which was followed by X-ray powder diffraction. *N*-Benzyl-*N*-methacryloylbenzoylformamide crystallized in a chiral space group, and the solid state reaction led to an optically active *β*-lactam via topochemically-controlled hydrogen abstraction by the alkenyl carbon atom. Photolysis of *N*-isopropyl-*N*-methacryloylbenzoylformamide in the solid state led to both oxetane formation and a transformation to azetidine-2,4-dione involving a 1,5-benzoyl shift.

Introduction

Solid state photoreaction has received much attention both from a mechanistic and synthetic perspective, because this reaction provides stereoselectivity as well as enantioselectivity for a wide range of products compared to reactions that occur in solution due to restriction of molecular movement imposed by the environment.[1−8] In addition, achiral substrates sometimes adopt a chiral orientation in the crystal lattice, even in the absence of any outside influences.[9,10] The chirality of such a molecule in the crystal can be transformed spontaneously through a solid state photoreaction into the stereocenter of the product. Therefore, the reactions in the solid phase may provide a model that will allow determination of origin of chirality in molecules of living matter.[11] As in the case of the absolute asymmetric synthesis by intermolecular 2 + 2 cycloaddition, several examples of successful intramolecular reactions have been reported.[12−19] Furthermore, elucidation of the relationship (1) between conformation of molecules and substituents, (2) between the space groups and substituents, and (3) between the arrangement of molecules in the crystal lattice and photoreactivity may play an important role in the fields of crystal engineering and organic asymmetric synthesis.

Another advantage associated with solid state photoreaction is that X-ray analysis allows the orientation of the constituent molecules to be determined prior to reaction and, in some favorable systems, even after the reaction has occurred. Schmidt et al. investigated bimolecular reactions in crystals through the crystallographic

† Chiba University.
‡ The University of Tsukuba.
§ Shinshu University.
⊗ Abstract published in *Advance ACS Abstracts,* August 1, 1997.

(1) Scheffer, J. R.; Garcia-Garibay, M.; Nalamasu, O. *Organic Photochemistry*; Padwa, A., Ed., Marcel Dekker: New York and Basel, 1987; Vol. 8, pp 249−338.
(2) Ramamurthy, V.; Weiss, R. G.; Hammond, G. S. *Advances in Photochemistry*, Vol. 18; Volman, D. H., Hammond, G. S., Neckers, D. C., Ed.; John Wiley & Sons: New York, 1993; pp 67−234.
(3) Ramamurthy, V.; Venkatesan, K. *Chem. Rev.* **1987**, *87*, 433−481.
(4) Zimmerman, H. E.; Zuraw, M. J. *J. Am. Chem. Soc.* **1995**, *117*, 5245−5262.
(5) Cohen, M. D.; Schmidt, G. M. *J. Chem. Soc.* **1964**, 1969.
(6) Venkatesan, K.; Ramamurthy, V. *Photochemistry in Organized and Constrained Media*; Ramamurthy, V., Ed.; VCH: New York, 1991; pp 133−184.
(7) Scheffer, J. R.; Pokkuluri, P. R. *Photochemistry in Organized and Constrained Media*; Ramamurthy, V., Ed., VCH: New York, 1991, pp 185−246.
(8) Vaida, M.; Popvitz-Biro, R.; Leiserowitz, L.; Lahav, M. *Photochemistry in Organized and Constrained Media*; Ramamurthy, V., Ed., VCH: New York, 1991, 247−302.
(9) Green B. S., Lahav, M.; Rabinovich, D. *Acc. Chem. Res.*, **1979**, *69*, 191−197.
(10) Sakamoto, M. *Chem. Eur. J.* **1997**, *3*, 684−689.
(11) Addadi, L.; Lahav, M. *Origin of Optically Activity in Nature*; Walker, D. C., Ed.; Elsevier: New York, 1979; Chapter 14.
(12) Sakamoto, M.; Hokari, N.; Takahashi, M.; Fujita, T.; Watanabe, S.; Iida, I.; Nishio, T. *J. Am. Chem. Soc.* **1993**, *115*, 818.
(13) We already reported the absolute oxetane synthesis by the solid state photoreaction of *N*-isopropyl-*N*-tigloylbenzoylformamide in preliminary form: Sakamoto, M.; Takahashi, M.; Fujita, T.; Watanabe, S.; Iida, I.; Nishio, T.; Aoyama, H. *J. Org. Chem.* **1993**, *58*, 3476−3477.
(14) For the absolute synthesis via radical pairs: Sakamoto, M.; Takahashi, M.; Fujita, T.; Iida, I.; Takehiko, N.; Watanabe, S. *J. Org. Chem.* **1995**, *60*, 4682−4683.
(15) For intramolecular hydrogen abstraction by carbonyl oxygen or thiocarbonyl sulfur: (a) Evans, S. V.; Garcia-Garibay, M.; Omkaram, N.; Scheffer, J. R.; Trotter, J.; Wireko, F. *J. Am. Chem. Soc.* **1986**, *108*, 5648−5649. (b) Sekine, A.; Hori, K.; Ohashi, Y.; Yagi, M.; Toda, F. *J. Am. Chem. Soc.* **1989**, *111*, 697−700. (c) Sakamoto, M.; Takahashi, M.; Shimizu, M.; Fujita T.; Takehiko, N.; Iida, I.; Yamaguchi K.; Watanabe, S. *J. Org. Chem.* **1995**, *60*, 7088−7089. (d) Hashizume, D.; Kogo, H.; Sekine, A.; Ohashi, Y.; Miyamoto, H.; Toda, F. *J. Chem. Soc., Perkin Trans. 2* **1996**, 61−66.
(16) For solid state di-*π*-methane rearrangement: (a) Garcia-Garibay, M.; Scheffer, J. R.; Trotter, J.; Wireko, F. *J. Am. Chem. Soc.* **1989**, *111*, 4985−4986. (b) Fu, T. Y.; Liu, Z; Scheffer, J. R.; Trotter, J. *J. Am. Chem. Soc.* **1993**, *115*, 12202−12203. (c) Roughton, A. L.; Muneer, M.; Demuth, M. *J. Am. Chem. Soc.* **1993**, *115*, 2085−2086.
(17) Sakamoto, M.; Takahashi, M.; Yamaguchi, K.; Fujita, T.; Watanabe, S. *J. Am. Chem. Soc.* **1996**, *118*, 8138−8139.
(18) Sakamoto, M.; Takahashi, M.; Kamiya, K.; Yamaguchi, K.; Fujita, T.; Watanabe, S. *J. Am. Chem. Soc.* **1996**, *118*, 10664−10665.
(19) Toda, F.; Tanaka, K. *Supramol. Chem.* **1994**, *3*, 87−88.

S0022-3263(97)00497-0 CCC: $14.00

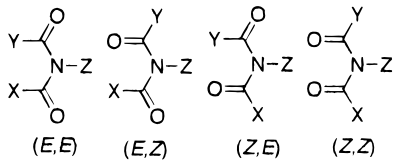

1: X = benzoyl group
Y = alkenyl group
Z = alkyl or aryl group

Figure 1.

Scheme 1

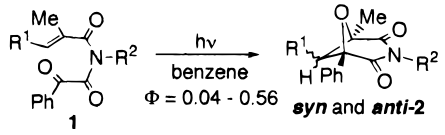

study of a large number of cinnamic acids. As a result, they developed an important set of "topochemical rules" with respect to photochemical reactivity by connecting the configuration of the product and the crystal structure of the reactant.[20]

The details of cyclobutane formation of alkenyl double bonds, di-π-methane rearrangement,[1,16] and the hydrogen transfer of carbonyl or alkenyl double bonds[1,21] have been studied extensively with respect to the geometric parameters of the reacting sites. However, the geometric parameters of the well-known Paterno−Büchi photocyclization (oxetane formation) are hitherto unknown. The present paper reports the photochemical behavior of *N*-(α,*β*-unsaturated carbonyl)benzoylformamides in the solid state and presents several remarkable examples of "absolute" asymmetric syntheses involving 2 + 2 oxetane formation and hydrogen transfer by the alkenyl carbon atom.

Results and Discussion

Acyclic imides, *N*-(α,*β*-unsaturated carbonyl)benzoylformamides **1**, were used in the photochemical study because they possess a nearly planar imide chromophore with photochemically reactive alkenyl and benzoyl groups at both ends of the imide carbonyls. Both chromophores were placed as close to each other as the appropriate conformation would allow. Irradiation of the imides **1** under homogeneous conditions results in cross-type 2 + 2 intramolecular cycloaddition between the ketone carbonyl and the alkenyl double bonds, the efficiency of which is dependent on the substituents (Scheme 1).[22] One important factor that determines the reactivity involves the distribution of the stable conformation of the imides. Conformations of asymmetric imides are described as (*E*,*E*), (*E*,*Z*), (*Z*,*E*) and (*Z*,*Z*), based on the planar sp^2 nitrogen atom (Figure 1). The energy barrier of rotation around the C(=O)−N bond is significantly lower (7−13 kcal/mol) than that of the corresponding amides (17−25 kcal/mol), reflecting the decreased C=N double bond characteristics of these systems. These conformational factors may play an important role in the photochemical reactivity of acyclic imides. Imides in the (*E*,*E*) conformation may be used for photochemical cycloaddition between benzoyl carbonyl (X) and alkenyl double bonds (Y). On the other hand, imides with an (*E*,*Z*), (*Z*,*E*), or (*Z*,*Z*) conformation cannot be used to produce oxetanes. Since the interconversion takes place in solution, most acyclic imides can promote oxetane formation, although the quantum efficiency is affected by the conformer distribution.

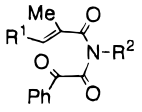

1

a: R^1 = Me, R^2 = Pr^i
b: R^1 = Me, R^2 = CH_2Ph
c: R^1 = Me, R^2 = Ph
d: R^1 = Me, R^2 = *o*-Tol
e: R^1 = Me, R^2 = 2,6-$Me_2C_6H_3$
f: R^1 = H, R^2 = R^2 = Pr^i
g: R^1 = H, R^2 = CH_2Ph
h: R^1 = H, R^2 = Ph
i: R^1 = H, R^2 = 2,6-$Me_2C_6H_3$
j: R^1 = H, R^2 = 2,6-$Cl_2C_6H_3$

Figure 2.

In the solid phase, conformational factors become more important because interconversion involving dramatic movement of the substituents cannot usually occur. Photoreactivity in the solid state cannot be determined only by the intramolecular parameter. In this case, although reorientation to permit the reaction to occur and the fitness of the surrounding crystal lattice are important considerations, two principal parameters, distance and the dihedral angle between the reacting carbonyl and the alkenyl double bonds, are the most critical for determining the photochemical reactivity of 2 + 2 cycloaddition.

Crystal Structure and the Conformation in the Crystalline State. The photochemical reaction of five *N*-tigloylbenzoylformamides **1a**−**e** and five *N*-methacryloylbenzoylformamides **1f**−**j** was studied both in solution and in a solid state (Figure 2). All imides except **1b** were subjected to X-ray single-crystal analysis.[29] The crystal data are summarized in Tables 1 and 2. Figure 3 shows the ORTEP diagram of the imides **1a** and **1c**−**1j**.

Table 3 shows the molecular conformation and the geometrical data of the imides **1**. All the imides showed an either *E*,*E* or *E*,*Z* conformation. In the *E*,*E* conformation, the reacting carbonyl and the alkenyl double bonds are assumed to be closely placed. Such imides are extremely useful for cross-type 2 + 2 cycloaddition. On the other hand, the *E*,*Z*-conformation is disadvantageous for cycloaddition because of the separation between the reacting double bonds. All imides maintain almost planer conformation for the imide plane, the torsional angles of the imide carbonyls, C1−N−C3−O3 or N−C1−C2−O2 are within 33° of the sp^2 nitrogen atom. The torsional angles of the alkenyl group against the N−C3−C4 plane are between 35.9° and 52.4°. Each carbonyl group of the benzoylformyl group twists in the range of 47.4° to 79.9°. The phenyl ring and carbonyl group of the benzoyl group are almost planar (absolute value: 3.0−13.3°). On the other hand, the aromatic rings on the nitrogen atom are nearly orthogonal to the imide chromophore (absolute value: 61.4−81.2°).

(20) Schmidt, G. H. J. *Pure Appl. Chem.* **1971**, *27*, 647.
(21) Wagner, P. J.; Park, B. *Organic Photochemistry*; Padwa, A., Ed., Marcel Dekker: New York and Basel, 1991; Vol. 11, pp 227−366.
(22) Sakamoto, M.; Aoyama, H.; Omote, Y. *J. Chem. Soc., Perkin Trans. 1* **1986**, 1759−1762.

Table 1. Crystal Data for *N*-(α,*β*-Unsaturated carbonyl)benzoylformamides 1a−e

entry	1a	1c	1d	1e
R^1	Me	Me	Me	Me
R^2	Pr^i	Ph	*o*-tolyl	2,6-$Me_2C_6H_3$
formula	$C_{16}H_{19}NO_3$	$C_{19}H_{17}NO_3$	$C_{20}H_{19}NO_3$	$C_{21}H_{21}NO_3$
mol weight	272.33	307.35	321.4	335.4
crystal system	monoclinic	orthorhombic	monoclinic	orthorhombic
space group	$P2_1$	$Pca2_1$	$P2_1/a$	$Pbca$
Z	2	4	4	8
a/Å	5.933(1)	9.271(4)	13.855(4)	13.543(5)
b/Å	12.552(1)	17.533(4)	20.352(5)	21.588(4)
c/Å	10.594(2)	10.320(5)	6.137(2)	12.526(5)
β/deg	100.35(1)	90[a]	102.17(2)	90[a]
V/Å^3	776.1	1677(2)	1691.6(8)	3662(1)
ρ_{calc}/g cm^{-3}	1.16	1.217	1.26	1.217
μ/cm^{-1}	0.8[b]	6.7[c]	6.48[c]	6.54[c]
F(000)	290	648	679	1424
crystal size/mm	0.4 × 0.15 × 0.20	0.05 × 0.05 × 0.50	0.50 × 0.15 × 0.15	0.30 × 0.30 × 1.00
used reflctns	2024	1480	2453	1817
R	0.052	0.038	0.0398	0.041
R_W	0.047	0.021	0.0435	0.035

[a] The angles of the crystal lattice are defined as $\beta = 90°$. [b] Mo Kα radiation was used. [c] Cu Kα radiation was used.

Table 2. Crystal Data for *N*-(α,*β*-Unsaturated carbonyl)benzoylformamides 1f−j

entry	1f	1g	1h	1i	1j
R^1	H	H	H	H	H
R^2	Pr^i	Bn	Ph	2,6-$Me_2C_6H_3$	2,6-$Cl_2C_6H_{32}$
formula	$C_{15}H_{17}NO_3$	$C_{19}H_{17}NO_3$	$C_{18}H_{15}NO_3$	$C_{20}H_{19}NO_3$	$C_{18}H_{13}NO_3Cl_2$
mol weight	259.3	307.35	293.32	321.38	362.21
crystal system	monoclinic	monoclinic	monoclinic	monoclinic	monoclinic
space group	$P2_1/a$	$P2_1$	$P2_1/c$	$P2_1/c$	$P2_1/c$
Z	4	2	4	4	4
a/Å	10.998(7)	9.649(5)	17.627(3)	8.533(3)	8.542(5)
b/Å	8.852(6)	8.318(3)	8.923(2)	11.184(3)	11.063(5)
c/Å	14.929(8)	10.216(5)	10.116(2)	18.845(2)	18.763(6)
β/deg	101.30(6)	98.05(2)	92.41(1)	100.80(2)	102.36(4)
V/Å^3	1425(1)	811.9	1589.8(5)	1766.5(8)	1731(1)
ρ_{calc}/g cm^{-3}	1.208	1.21	1.23	1.208	1.389
μ/cm^{-1}	6.51[a]	0.8[b]	6.466[a]	6.57[a]	35.1[a]
F(000)	552	312	615	680	744
crystal size /mm	0.50 × 0.50 × 0.50	0.70 × 0.50 × 0.60	0.30 × 0.35 × 0.20	0.50 × 0.30 × 0.70	0.50 × 0.50 × 1.00
used reflctns R	1587	2290	2234	2038	2220
R	0.069	0.041	0.0554	0.045	0.047
R_W	0.068	0.042	0.061	0.039	0.05

[a] Cu Kα radiation was used. [b] Mo Kα radiation was used.

Determination of the Conformation of (*E*,*E*) or (*E*,*Z*) Imides in the Crystalline states. The relationship between the substituents and the conformation of the imide moiety is rather complex. The intermolecular interaction due to the crystal packing force is one of the most important factors in the crystals. A consistent relationship does not appear to exist between the molecular conformation and the substituents based solely on the intramolecular interaction. However, the intramolecular interaction of each chromophore may play an important role in determining the conformation. Recent work has suggested the existence of an interaction between the C−H group and the π-electron system on the basis of the conformational relationship associated with a series of compounds that bear an aliphatic group on one side of the molecule and a phenyl group on another.[23] X-ray and photochemical results indicate that tigloyl derivatives **1a-e** except **1c** prefer the (*E*,*E*) conformation. The ORTEP diagrams indicate that the CH$\cdots\pi$ interaction between the β-methyl group and benzoyl phenyl ring restrains the molecular conformation. As a result, the distance between the β-methyl hydrogen atom and the center of phenyl ring is 3.37 Å for **1a**, 2.98 Å for **1d**, and 3.16 Å for **1e**.[24]

Of the methacryloyl derivatives (**1f−j**), only the isopropyl derivative (**1f**) crystallized in the (*E*,*E*) conformation. The others crystallized in the (*E*,*Z*) conformation. Intramolecular interaction was not found in the crystal of **1c**. On the other hand, the alkenyl group and phenyl ring were in closer proximity in the *N*-aryl derivatives, and therefore this interaction may play an important role in determining the molecular conformation; the distance between the alkenyl group and the edge of the benzene ring was 3.26 Å for **1h**, 3.38 Å for **1i**, and 2.96 Å for **1j**.

Photochemical Reaction of the Imides 1a−j in Solution. We already reported that irradiation of **1f** and **1g** in benzene underwent [2 + 2] cyclization to bicyclic oxetanes **2f** and **2g** in 96% and 99% yields, respectively.[22] Photolysis of other imides in benzene also gave corresponding oxetanes in high yields as shown in Table 4. In the case of tigloyl derivatives **1a−1e**, oxetanes were obtained as a mixture of two stereoisomers. The ratio of ***syn*-2**/***anti*-2** was 2.1, independent of the substituents on the nitrogen atom. The stereochemistry was determined on the basis of NOE experiments. Furtheremore, the structure was established by X-ray single-crystal analysis of ***syn*-2a**.

(23) Nishio, M; Umezawa, Y.; Hirota, M.; Takeuchi, Y. *Tetrahedron* **1995**, *51*, 8665−8701.

(24) Jorgensen, W.; Seberance, L. *J. Am. Chem. Soc.* **1990**, *112*, 4768−4777.

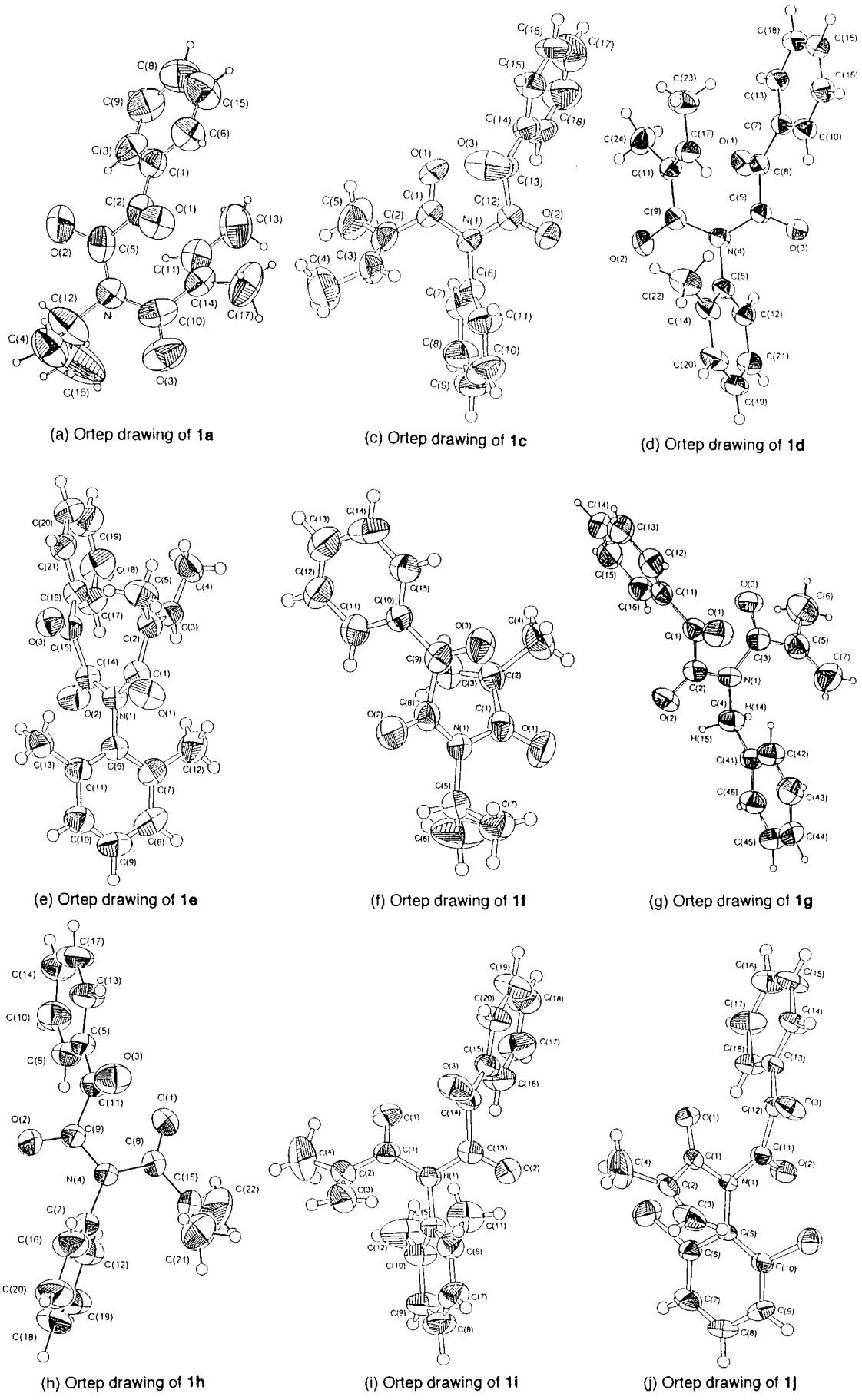

Figure 3. ORTEP drawings of the X-ray structures of **1a-1j**.

Photochemical Reaction of Imides with the Tigloyl Group (1a−e) in the Solid State. All crystals are recrystallized from chloroform−hexane solution and were photolyzed as powders sandwiched between Pyrex

Table 3. Conformation of Imides 1 and the Torsional Angles

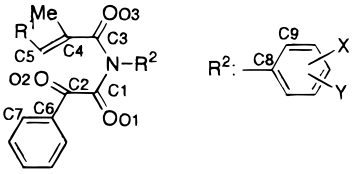

1	conformation	C1−N−C3−O3	C3−N−C1−O1	N−C1−C2−O2	N−C3−C4−C5	O2−C2−C6−C7	C1−N−C8−C9
1a	*E,E*	150.4	−178.3	−60.5	−46.8	−7.5	*a*
1c	*E,Z*	15.5	−168.0	72.0	50.4	3.0	62.9
1d	*E,E*	155.5	172.6	−54.0	−47.3	8.6	−77.9
1e	*E,E*	157.9	173.6	−56.8	−48.2	13.3	98.8
1f	*E,E*	147.0	179.5	−47.4	−35.9	−8.4	*a*
1g	*E,Z*	−4.0	168.4	−76.9	−52.4	−9.1	*a*
1h	*E,Z*	−8.7	166.4	−72.4	−56.3	−9.0	−69.0
1i	*E,Z*	−2.6	163.2	−79.9	−46.6	3.5	−75.9
1j	*E,Z*	−15.0	160.0	−55.0	−36.9	4.9	−74.0

[a] R^2 is not an aryl group.

Table 4. Photolysis of Imides 1a−j in Benzene

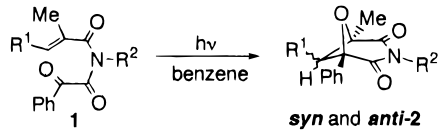

entry	yield of **2**, % (*syn*/*anti*)
1a	100 (2.1)
1b	100 (2.1)
1c	76 (2.1)
1d	100 (2.1)
1e	100 (2.1)
1f	96
1g	99
1h	100
1i	100
1j	100

glasses on the inside of a polyethylene bag with a 500-W high-pressure mercury lamp.

When the powdered crystals of **1a** were photolyzed at 0 °C for 1 h, bicyclic oxetane **2a** was obtained as a mixture of stereoisomers in 84% yield at a ratio of ***syn*-2a**/***anti*-2a** = 3.7. X-ray crystal structural analysis of **1a** indicated that the space group is chiral $P2_1$ (Table 1). As expected, the major isomer ***syn*-2a** showed optical activity, $[\alpha]^{20}_D$ +34 (*c* 1.0 in $CHCl_3$), 35% ee (conversion 100%), whereas the minor isomer ***anti*-2a** was obtained as a racemate. Unfortunately, the crystals melted during irradiation under these conditions. The solid state photoreaction proceeded, even at −78 °C, yielding the optically active (+)-***syn*-2a** which showed a higher ee value, $[\alpha]^{20}_D$ +95 (*c* 1.0 in $CHCl_3$), >99% ee (conversion 100%, chemical yield 89%, ***syn*-2a**/***anti*-2a** = 6.7).

To explain how the *anti* isomer was produced as a racemate, the time course for consumption of **1a** and the formation of **2a** (*syn* and *anti* isomers) was studied (Figure 4). When **1a** was irradiated in benzene, the yield of **2a** showed a roughly linear increase from the initial stage at the expense of **1a**. During photolysis, *trans*-**1a** was not detected at all, and both ***syn*-2a** and ***anti*-2a** were formed constantly at ***syn*-2a**/***anti*-2a** = 2.1 throughout the reaction, even after all **1a** was consumed. Thus, the photoreaction appears to proceed via a diradical intermediate (**3a**), and the direct *cis-trans* isomerization of **1a** and the back reaction from **3a** to **1a** does not occur, as depicted in Scheme 2. On the basis of these assumptions, racemic ***anti*-2a** is obtained as a result of the solid state photoreaction due to the partial

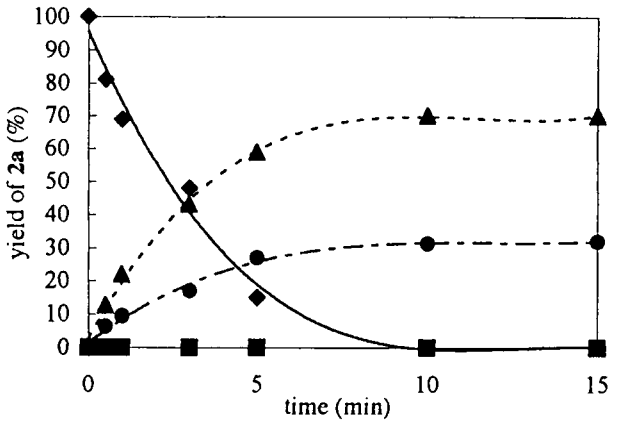

Figure 4. Time course for the photoreaction of *cis*-**1a** (◆) and the formation of *trans*-**1a** (■), *syn*-**2a** (▲), and *anti*-**2a** (●) in benzene solution.

Scheme 2

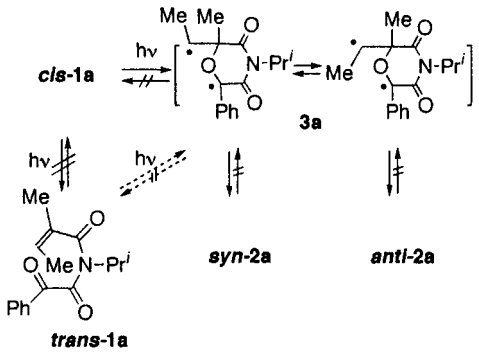

racemization which takes place at the defect lattice sites where ***anti*-2a** is formed.

The absolute configuration of (+)-**2a** was determined by an indirect method to be (1*R*,5*R*,7*R*)-1,7-dimethyl-3-isopropyl-5-phenyl-6-oxa-3-azabicyclo[3.1.1]heptane-2,4-dione. That of thiocarbonyl derivative (−)-***syn*-4a** obtained by thionation of (+)-***syn*-2a** was determined by X-ray crystallographic analysis using anomalous scattering method to be (1*R*,5*R*,7*R*)-1,7-dimethyl-3-isopropyl-5-phenyl-4-oxo-6-oxa-3-azabicyclo[3.1.1]heptane-2-thione (Scheme 3). Direct determination of the absolute configuration of **1a** in the chiral crystal could not be performed. However, it is reasonably concluded that one enantiomorph, which yielded (+)-***syn*-2a** by the solid state photolysis, should be consistent with the ***M*** configuration shown in Figure 3a and Scheme 3.

Scheme 3

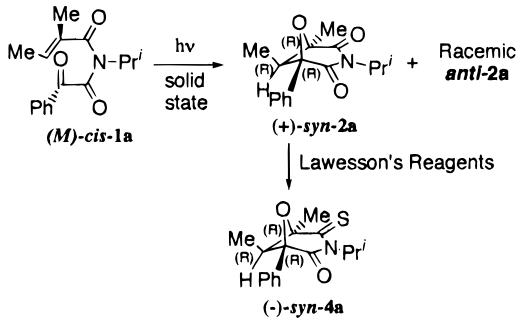

Table 5. Photolysis of Imides 1a–j in the Solid State

entry	reactn temp (°C)	yield of **2**, % (*syn*/*anti*)	ee (%)
1a	0	84 (3.7)	35[a]
1a	−78	89 (6.7)	99[a]
1b	15	100 (60)	91[a]
1b	−78	100 (60)	91[a]
1c	0	0[b]	
1d	15	100 (27)	0
1e	15	100 (20)	0
1f	0	68 (31)[c]	0
1g	0	50 (15)[d]	0 (88)[e]
1h	15	0[f]	
1i	15	0[f]	
1j	15	0[f]	

[a] ee of ***syn*-2**. [b] Only *cis*–*trans* isomerization took place and the ratio of ***cis*-1c**/***trans*-1c** was 1.3. [c] Chemical yield of **5f**. [d] Chemical yield of **6g**. [e] ee of **6g**. [f] Starting materials were recovered.

Solid state photolysis of **1b** also yielded oxetane **2b**, but the reaction proceeded more stereoselectively than that of **1a** with the ratio of *syn*/*anti* = 60 (Table 5). Unfortunately, a single crystal could not be obtained from **1b** for X-ray single-crystal analysis. However, the crystal-to-crystal transformation was followed by X-ray powder diffraction. Figure 5 shows the diffraction patterns which indicate that the transformation proceeds effectively to oxetane **2b** while retaining a crystal lattice (F-2). After 30 min, all of the starting material changed to oxetane (F-3). F-4 shows the diffraction pattern that differs from that of recrystallized oxetane **2b**. This indicates that photolyzed crystals are metastable.

Whereas the space group of **1b** was ambiguous, oxetane ***syn*-2b** obtained by solid state photolysis at 15 °C was optically active, $[\alpha]^{20}_D = +57$, 91% ee as shown in Table 5. Low-temperature photolysis (−78 °C) produced similar results in which there was no change in the ratio of ***syn*-2b**/***anti*-2b** or the ee value because the solid state reaction proceeded *via* the crystal-to-crystal path, even at room temperature. Enantiomorphic **1b** was also obtained by spontaneous resolution, and both enantiomers were synthesized selectively by the seeding method.

Solid state photolysis of **1c** showed that the crystal differed remarkably from **1a** and **1b** with respect to photochemical behavior. X-ray single-crystal analysis revealed that the crystal was a orthorhombic achiral space group $Pca2_1$ with an (*E*,*Z*) conformation which is disadvantageous for oxetane formation (Figure 3c). In this case, oxetane was not obtained but a photostationary state of ***cis*-1c**/***trans*-1c** = 1.3 was obtained.[1,25] Photochemical *cis*–*trans* isomerization was also observed in the benzene solution during the early stage of the reaction (*cis*/*trans* = 1.4). Since structural modification resulting from rotation of the C(=O)–N bond from (*E*,*Z*) to (*E*,*E*) is allowed in solution, the following two reactions occur competitively: (a) *cis*–*trans* isomerization and (b) oxetane formation from an (*E*,*E*) conformer.

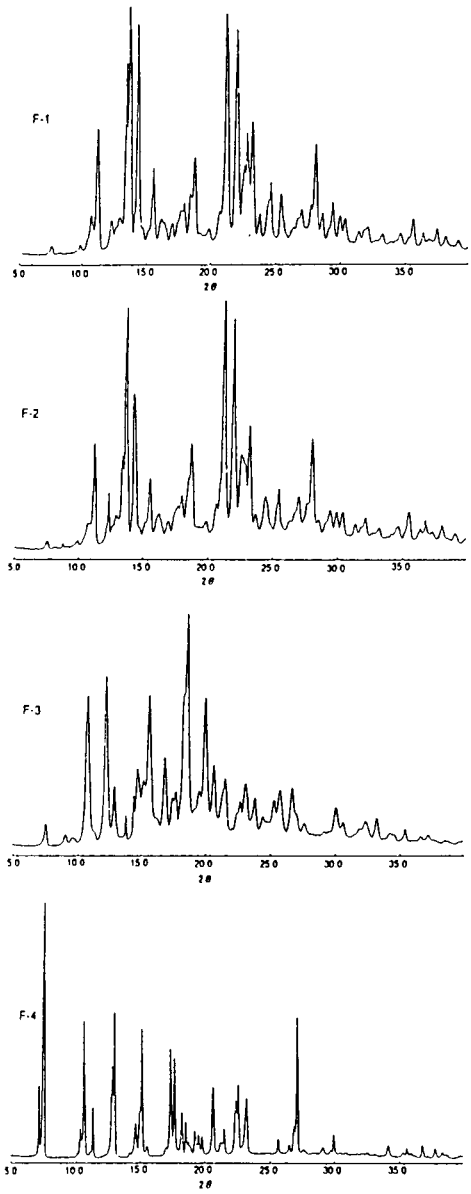

Figure 5. X-ray diffraction patterns for the transformation of **1b** to **2b**. (F-1) Starting material **1b**. (F-2) Irradiated for 5 min. (F-3) Irradiated for 30 min. (F-4) Recrystallized **2b** from $CHCl_3$–hexane.

As expected from X-ray analysis, solid state photolysis of **1d** yielded racemic oxetane **2d** in a 100% yield (*syn*/*anti* = 27). Photolysis of **1e** also yielded racemic oxetane **2e** in the ratio of *syn*/*anti* = 20. In both cases, the crystal-to-crystal transformations were observed and followed by X-ray powder diffraction. Figures 6 and 7 show the diffraction patterns of solid state photolysis of **1d** and **1e**. These indicate that the transformation progressed effectively to oxetanes **2d** and **2e** while retaining a crystal lattice.

Photochemical Reaction of Imides with the Methacryloyl group (1f–j) in the Solid State. X-ray crystallographic analysis of **1f** revealed that the molecular conformation was (*E*,*E*) and the space group was achiral, $P2_1/a$ (Table 2, Figure 3f). The molecular conformation in the crystal is suitable for oxetane formation.

(25) Kinbara, K.; Saigo, K. *Bull. Chem. Soc. Jpn.* **1996**, *69*, 779–784 and references cited therein.

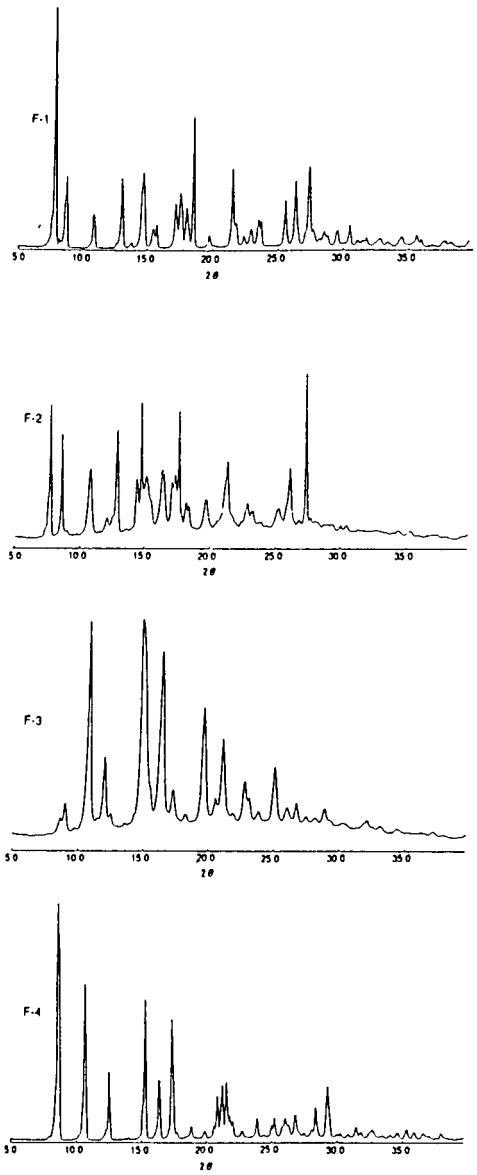

Figure 6. X-ray diffraction patterns for the transformation of **1d** to **2d**. (F-1) Starting material **1d**. (F-2) Transition pattern. (F-3) Irradiated crystals (100% conversion). (F-4) Recrystallized **2d** from $CHCl_3$−hexane.

When the crystals were irradiated in the solid state, the corresponding oxetane **2f** was obtained as well as an unexpected product, azetidine-2,4-dione **5f** in 68% and 31% yields, respectively (Scheme 4).

The formation of **5f** can be explained in terms of cyclization that results in 1,4-diradical formation by an α-cleavage reaction that involves a 1,5-benzoyl shift.[26] The (*E*,*E*) conformation is also preferred for the 1,5-benzoyl shift. The distance between carbonyl carbon C9 and alkenyl β-carbon C3 was 2.84 Å, which is shorter than the sum of the van der Waals radii (3.0 Å). Figure 8 shows the correlation between the conversion rates and chemical yields of **2f** and **5f** in the solid state photoreaction at 0 °C. The photolysate melts at a conversion rate of approximately 50%. During this process, the photolyzed crystals maintained the crystalline phase and the yields of both **2f** and **5f** increased as a result of the increased conversion. After the crystals melt, only oxetane was obtained. These results indicate that the topochemically-allowable solid state photoreaction dominates both the 1,5-benzoyl shift and oxetane formation.

(26) Aoyama, H.; Sakamoto, M.; Omote, Y. *J. Chem. Soc., Chem. Commun.* **1982**, 119−120.

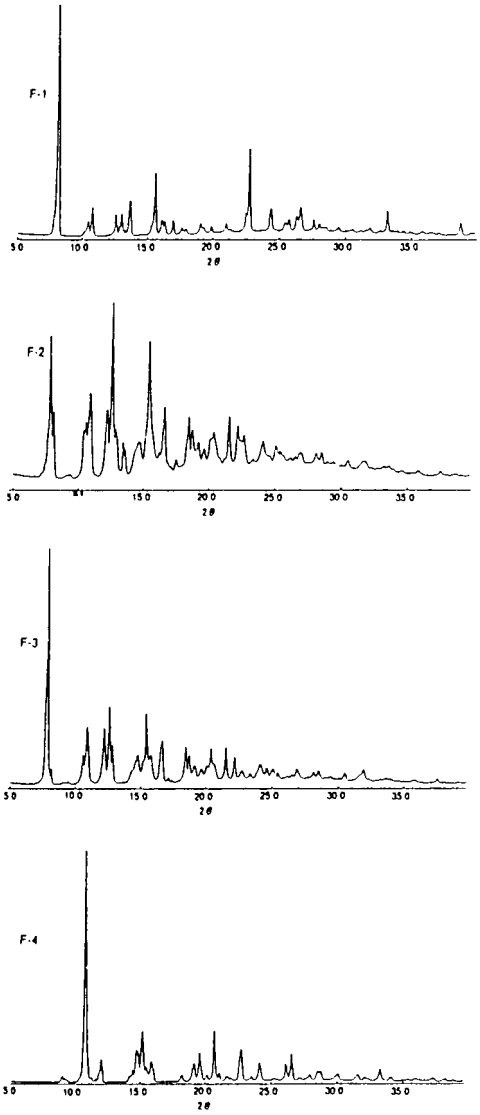

Figure 7. X-ray diffraction patterns for the transformation of **1e** to **2e**. (F-1) Starting material **1e**. (F-2) Transition pattern. (F-3) Irradiated crystals (100% conversion). (F-4) Recrystallized **2e** from $CHCl_3$-hexane.

Scheme 4

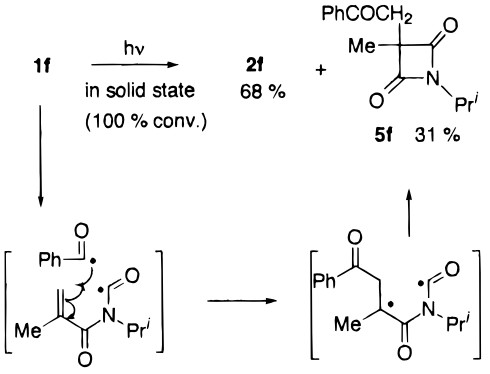

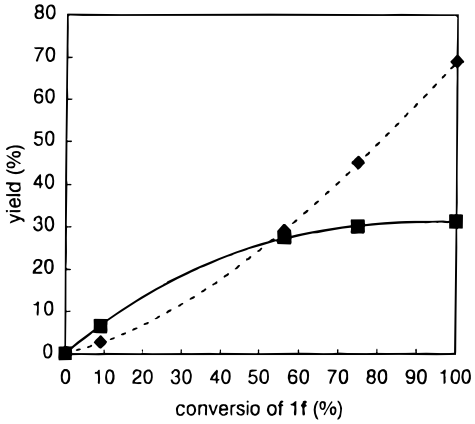

Figure 8. Correlation diagram between the conversion and the chemical yields of **2f** (◆) and **5f** (■) in the solid state photolysis at 0 °C.

Scheme 5

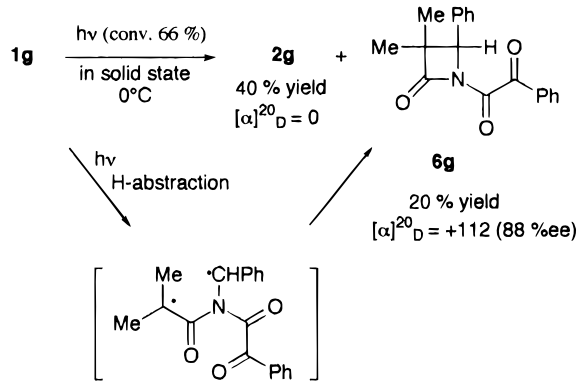

both **2g** and a topochemical product, azetidin-2-one **6g**, in 40% and 20% yields, respectively, at a 66% conversion rate (Scheme 5). X-ray crystallographic analysis of **1g** shows that the space group of the crystal was chiral, $P2_1$ (Table 2), and isolated azetidin-2-one **6g** exhibited optical activity $[\alpha]^{20}_D = +112$, 88% ee. However, oxetane **2g** that possesses two chiral centers was obtained as a racemate.

The mechanism associated with the transformation of **1g** to **6g** can be reasonably explained in terms of hydrogen abstraction by the alkenyl carbon leading to a 1,4-biradical (Scheme 5).[27,28] The ORTEP diagram shows that the conformation of the imide chromophore was (*E*,*Z*), which is disadvantageous for oxetane formation (Figure 3). Formation of **2g** requires structural modification from an (*E*,*Z*) to (*E*,*E*) conformation, which is impossible to perform in the crystalline state. Figure 9 shows the time course for the chemical yields of both **2g** and **6g** and that of the ee value for **6g** versus the conversion of **1g**. At the early stage of the reaction, azetidinone **6g** was formed preferentially. As the conversion rate increased, formation of oxetane **2g** became accelerated. Throughout the reaction, the ee value of the resultant azetidinone ranges from 85% to 88% within the acceptable experimental error whereas that of oxetane was zero. On the basis of these results, the formation of

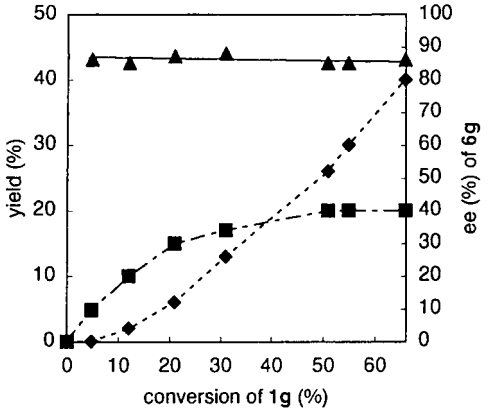

Figure 9. Correlation diagram of the conversion of **1g** versus the chemical yields of 2g (◆) and **6g** (■). (△) ee of **6g**.

azetidinone via hydrogen transfer by the alkenyl carbon atom is a topochemically-controlled process. Furthermore, oxetane **2g** was formed in the defect crystal lattice in which the (*E*,*Z*) conformation changed to the energetically more stable (*E*,*E*) conformation. Therefore, racemic oxetane **2g** was obtained during solid state photolysis, even in the chiral crystal environment. The same phenomenon was observed during solid state photolysis of **1a** in which racemic ***anti*-2a** was formed after the chirality of the crystal was no longer apparent.

Scheffer et al. examined the solid state hydrogen transfer by the alkenyl carbon atom and defined the important geometrical parameters of the hydrogen transfer reaction.[1] In the case of **1g**, conformation in the crystalline state is apparently advantageous for the formation of azetidinone **6g** (Figure 3). The angle between the P_z orbital of alkenyl carbon C7 and the benzylic hydrogen atom (H14) was 64.8° (ideal 90°), and the intramolecular distance between the C7 and the H14 was 2.61 Å which is much shorter than the sum of the van der Waals radii (2.90 Å).

Photolysis of imides **1h**−**j** in benzene solution yielded the corresponding oxetanes in quantitative amounts. However, crystals of the imides were nonreactive to photolysis. This poor reactivity may be explained on the basis of the molecular conformation in the solid state (Figures 3h−j). X-ray crystallographic analysis of **1h**, **1i**, and **1j** revealed that all the crystals are members of the monoclinic space group $P2_1/c$ and the conformation was (*E*,*Z*) which is disadvantageous for oxetane formation.

Relationship between the Conformation of the Imides and Photoreactivity. Table 6 shows the relationship between the molecular conformation and the geometric parameters of the reacting carbonyl and alkenyl double bonds for oxetane formation. In the (*E*,*E*) conformation, the double bonds are maintained in close proximity, such that the distance between the reacting carbonyl oxygen and alkenyl carbon is 2.8−3.1 Å and that between carbonyl carbon and the alkenyl carbon is 2.8−3.0 Å. In this case, the double bonds are almost parallel (dihedral angle < 23°). In the (*E*,*Z*) conformation, the molecules are unreactive to oxetane formation, and the distance between carbonyl oxygen and alkenyl carbon is 4.5−4.8 Å, which is considerably longer than the sum of the van der Waals radii (3.22 Å). Furthermore, the reacting carbonyl carbon and alkenyl carbon atoms exceed the sum of the van der Waals radii (3.4 Å) by a considerable margin. Photochemical reactivity was primarily influenced by the conformation of the imide chromophore.

(27) Aoyama, H.; Hasegawa, T.; Okazaki, M. *J. Chem. Soc., Perkin Trans. 1* **1979**, 263−268.
(28) Sakamoto, M.; Kimura, M.; Shimoto, T.; Fujita, T.; Watanabe, S. *J. Chem. Soc., Chem. Commun.* **1990**, 1214−1215.
(29) The author has deposited atomic coordinates for structures **1a,c-j**, *syn*-**2a**, and *syn*-**4a** with the Cambridge Crystallographic Data Centre. The coordinates can be obtained, on request, from the Director, Cambridge Crystallographic Data Centre, 12 Union Road, Cambridge, CB2 1EZ, UK.

Table 6. Geometrical Parameter for the Oxetane Formation

1	conformation	distance between reacting atoms C···O[b]	distance between reacting atoms C···C[c]	dihedral angle of C=O and C=C[d]
1a	*E*,*E*	2.98	2.99	22.9
1b	*E*,*E*[a]			
1c	*E*,*Z*	3.79	4.75	36.0
1d	*E*,*E*	2.68	2.70	23.3
1e	*E*,*E*	2.98	2.98	23.4
1f	*E*,*E*	2.78	2.84	20.6
1g	*E*,*Z*	4.71	5.28	31.7
1h	*E*,*Z*	4.50	4.91	33.6
1i	*E*,*Z*	4.47	5.19	34.3
1j	*E*,*Z*	4.54	5.18	41.0

[a] The conformation was speculated from the experimental results. [b] Distance between the reacting alkenyl β-carbon and the benzoyl carbonyl oxygen atoms. [c] Distance between the reacting alkenyl α-carbon and the benzoyl carbonyl carbon atoms. [d] Dihedral angle of the reacting double bond.

Conclusion

Photolysis of the ten *N*-(α,β-unsaturated carbonyl)benzoylformamides yielded cross-type oxetanes under homogeneous conditions. In contrast, irradiation of these compounds in the solid state resulted in a considerably different photochemical behavior in which the molecular conformation in the crystalline phase reflected the photoreactivity and photoproducts. New topochemically-controlled reactions observed during azetidine-2,4-dione formation and hydrogen abstraction by the alkenyl carbon atom are reactions that can only be observed in the solid state. Three of the ten achiral imides yielded chiral crystals by spontaneous resolution. The solid state photolysis yielded optically active compounds. These reactions provide two examples of absolute asymmetric synthesis, oxetane formation by intramolecular 2 + 2 cycloaddition and β-lactam synthesis from the hydrogen abstraction by an alkenyl carbon atom.

Experimental Section

General. NMR spectra were recorded on $CDCl_3$ solutions on a JEOL FX-270, GSX-400, and GSX-500 operating at 270, 400, or 500 MHz are referenced to 0 ppm relative to TMS as internal standard. Elemental analyses were made using a Perkin-Elmer-240 instrument. IR spectra were recorded on JASCO IR-420 or FT/IR-230 spectrometers as KBr disks, unless otherwise noted. Optical rotations were determined on a JASCO DIP-370 polarimeter operating at the sodium D line in $CHCl_3$ solution at the concentration of $c = 1.0$.

General Procedure for the Preparation of *N*-(α,β-Unsaturated carbonyl)benzoylformamides 1a−j. All *N*-(α,β-unsaturated carbonyl)benzoylformamides **1a**−**j** were prepared by the condensation of benzoylformyl chloride and corresponding α,β-unsaturated amides in the presence of triethylamine according to the literature.[22] The structures of the imides **1a**−**e**, **1h**, and **1j** were determined on the basis of spectral data. Those of imides **1f**, **1g**, and **1i**, were confirmed by the comparison of the spectral data cited in the literature.

***N*-Isopropyl-*N*-tigloylbenzoylformamide (1a)** was obtained as a colorless needle crystal: yield 75%; mp 65−66 °C; IR (cm^{-1}, KBr) 1650, 1710; UV (nm, CH_3CN) 256 (ϵ 11 600), 351 (ϵ 140); ^1H NMR ($CDCl_3$) δ 1.05 (qd, J = 0.7 and 6.8 Hz, 3H), 1.47 (d, J = 7.0 Hz, 6H), 1.60 (brs, 3H), 4.78 (sept, J = 7.0 Hz, 1H), 6.03 (dq, J = 0.7 and 6.8 Hz, 1H), 7.4−7.7 (m, 3H), 7.9−8.0 (m, 2H); ^{13}C NMR ($CDCl_3$) δ 12.5 (q), 13.0 (q), 19.6 (q), 48.2 (d), 128.7 (d), 129.6 (d), 132.9 (s), 134.2 (d), 137.5 (d), 138.3 (s), 168.8 (s), 174.4 (s), 186.4 (s). Anal. Calcd for $C_{16}H_{19}O_3N$: C, 70.31; H, 7.01; N, 5.12. Found: C, 70.50; H, 6.98; N, 5.04.

***N*-Benzyl-*N*-tigloylbenzoylformamide (1b)** was obtained as a colorless powder: yield 80%; mp 44−45 °C; IR (cm^{-1}, KBr) 1660, 1640, 1710; UV (nm, CH_3CN) 257 (ϵ 7000), 346 (ϵ 40); ^1H NMR ($CDCl_3$) δ 0.98 (qd, J = 1.0 and 6.6 Hz, 3H), 1.62 (brs, 3H), 5.06 (s, 2H), 5.82 (dq, J = 1.0 and 6.6 Hz, 1H), 7.2−7.6 (m, 8H), 7.9−8.0 (m, 2H); ^{13}C NMR ($CDCl_3$) δ 12.7 (q), 46.9 (t), 127.7 (d), 128.3 (d), 128.6 (d), 128.8 (d), 129.5 (d), 134.4 (d), 136.4 (s), 136.5 (d), 132.8 (s), 137.0 (s), 169.1 (s), 173.8 (s), 185.9 (s). Anal. Calcd for $C_{20}H_{19}O_3N$: C, 74.73; H, 5.96; N, 4.36. Found: C, 74.65; H, 6.02; N, 4.32.

***N*-Tigloylbenzoylformanilide (1c)** was obtained as a colorless prismatic crystal: yield 78%; mp 91−92 °C; IR (cm^{-1}, KBr) 1670, 1690; UV (nm, CH_3CN) 250 (ϵ 15 100), 350 (ϵ 90); ^1H NMR ($CDCl_3$) δ 1.46 (qd, J = 1.0 and 6.9 Hz, 3H), 1.62 (brs, 3H), 6.40 (dq, J = 1.0, 6.9 Hz, 1H), 7.2−7.7 (m, 7H), 8.0−8.1 (m, 2H); ^{13}C NMR ($CDCl_3$) δ 12.7 (q), 13.9 (q), 127.6 (d), 128.5 (d), 128.7 (d), 129.3 (s), 129.5 (d), 129.8 (d), 132.8 (s), 139.6 (d), 132.9 (s), 134.2 (d), 169.6 (s), 173.9 (s), 187.2 (s). Anal. Calcd for $C_{19}H_{17}O_3N$: C, 74.20; H, 5.57; N, 4.56. Found: C, 74.20; H, 5.36; N, 4.48.

***N*-Tigloylbenzoyl-*o*-methylformanilide (1d)** was obtained as a colorless prismatic crystal: yield 72%; mp 77−78 °C; IR (cm^{-1}, KBr) 1640, 1670, 1710; UV (nm, CH_3CN) 210 (ϵ 24 800), 251 (ϵ 12 300), 336 (ϵ 170); ^1H NMR ($CDCl_3$) δ 1.38 (qd, J = 1.0 and 6.8 Hz, 3H), 1.62 (brs, 3H), 2.31 (s, 3H), 6.31 (dq, J = 1.0 and 6.8 Hz, 1H), 7.1−7.7 (m, 7H), 8.0−8.1 (m, 2H); ^{13}C NMR ($CDCl_3$) δ 12.7 (q), 13.7 (q), 17.7 (s), 127.0 (d), 128.3 (d), 128.8 (d), 129.1 (d), 129.7 (d), 131.5 (d), 132.8 (s), 133.5 (s), 134.2 (d), 135.6 (s), 136.1 (s), 138.2 (d), 169.6 (s), 173.6 (s), 186.8 (s). Anal. Calcd for $C_{20}H_{19}O_3N$: C, 74.58; H, 5.92; N, 4.35. Found: C, 74.75; H, 5.96; N, 4.36.

***N*-Tigloylbenzoyl-2,6-dimethylformanilide (1e)** was obtained as a colorless prismatic crystal: yield 75%; mp 106−107 °C; IR (cm^{-1}, KBr) 1670, 1715; UV (nm, CH_3CN) 254 (ϵ 11 600), 339 (ϵ 130); ^1H NMR ($CDCl_3$) δ 1.28 (qd, J = 1.3 and 6.9 Hz, 3H), 1.65 (d, J = 1.3 Hz, 3H), 2.29 (s, 6H), 6.24 (dq, J = 1.3, 6.9 Hz, 1H), 7.1−7.7 (m, 6H), 7.9−8.1 (m, 2H); ^{13}C NMR ($CDCl_3$) δ 12.8 (q), 13.5 (q), 18.1 (s), 128.8 (d), 128.9 (d), 129.1 (d), 129.6 (d), 132.9 (s), 134.2 (d), 136.2 (s), 137.1 (d), 169.8 (s), 173.0 (s), 186.5 (s). Anal. Calcd for $C_{21}H_{21}O_3N$: C, 75.19; H, 6.31; N, 4.18. Found: C, 75.04; H, 6.29; N, 4.13.

***N*-Methacryloylbenzoylformanilide (1h)** was obtained as a colorless prismatic crystal: yield 72%; mp 101−102 °C; IR (cm^{-1}, KBr) 1675, 1700, 1710; UV (nm, CH_3CN) 252 (ϵ 15 500), 336 (ϵ 170); ^1H NMR ($CDCl_3$) δ 1.77 (d, J = 1.3 Hz, 3H), 5.42 (d, J = 1.3 Hz, 1H), 5.58 (brs, 1H), 7.2−7.7 (m, 8H), 7.9−8.1 (m, 2H); ^{13}C NMR ($CDCl_3$) δ 18.7 (q), 126.4 (t,), 127.7 (d), 128.8 (d), 129.6 (d), 129.8 (d), 132.8 (s), 134.3 (d), 136.6 (s), 139.1 (s), 169.8 (s), 173.1 (s), 187.2 (s). Anal. Calcd for $C_{18}H_{15}O_3N$: C, 73.79; H, 5.12; N, 4.78. Found: C, 73.63; H, 5.03; N, 4.72.

***N*-Methacryloylbenzoyl-2,6-dichloroformanilide (1j)** was obtained as a colorless prismatic crystal: yield 70%; mp 125−126 °C; IR (cm^{-1}, KBr) 1680, 1690, 1720; UV (nm, CH_3CN) 252 (ϵ 14 500); ^1H NMR ($CDCl_3$) δ 1.90 (d, J = 1.3 Hz, 3H), 5.37 (d, J = 1.3 Hz, 1H), 5.58 (br s, 1H), 7.2−7.7 (m, 6H), 7.9−8.1 (m, 2H); ^{13}C NMR ($CDCl_3$) δ 18.8 (q), 124.0 (t), 128.8 (d), 129.1 (d), 129.7 (d), 130.8 (d), 132.8 (s), 133.0 (s), 135.0 (s), 168.6 (s), 171.6 (s), 185.8 (s). Anal. Calcd for $C_{18}H_{13}O_3NCl_2$: C, 59.83; H, 3.63; N, 3.88. Found: C, 59.91; H, 3.67; N, 3.79.

General Procedure for the Photochemical Reaction in Benzene. A benzene solution of imides **1a**−**1j** (0.02 M/L) was purged with deoxygenated and dried argon for 15 min prior to photolysis and irradiation with a 500-W high-pressure mercury lamp through a Pyrex filter. After irradiation, the photolysate was chromatographed using Merk kieseigel 60 with benzene as the eluent. Crystalline products were recrystallized from a chloroform−hexane mixture.

General Procedure for the Photochemical Reaction in the Solid State. All of the solid state photolyses were done under an atmosphere of deoxygenated and dried nitrogen. Solid samples were irradiated as powders sandwiched between Pyrex glasses on the inside of polyethylene bags and were fixed outside of an emersion well apparatus and cooled during the photolysis in either a water bath (15 °C) or an ice-water bath

(at 0 °C). Sandwiched glasses incorporated into Pyrex tubes were used for the solid state photolysis at −78 °C with a dry ice/methanol bath. After irradiation, the photolysate was treated in the same way as the photoreaction in solution.

Irradiation of *N*-Isopropyl-*N*-tigloylbenzoylformamide (1a.) After irradiation of a benzene solution (0.02 M) at 100% conversion, one fraction was isolated as an oil in a 100% yield by column chromatography on silica gel. An ^{1}H NMR spectrum revealed that it was composed of a mixture of two stereoisomers (2.1:1). Each stereoisomer was separated by preparative HPLC using Capcell Pak C18 (Shiseido) with MeCN/H_2O = 4:1 as eluent. The enantiomeric purity was determined by ^{1}H NMR spectroscopy employing 0.3 equiv of Eu(hfc)$_3$ (Aldrich).

***syn*-1,7-Dimethyl-3-isopropyl-5-phenyl-6-oxa-3-azabicyclo[3.1.1]heptane-2,4-dione (*syn*-2a)** (major isomer): mp 112−113 °C; IR (cm^{-1}, KBr) 1685, 1745; UV (nm, CH_3CN) 257 (ϵ 550); ^{1}H NMR ($CDCl_3$) δ 1.05 (d, J = 7.0 Hz, 3H), 1.45 (d, J = 7.0 Hz, 3H), 1.46 (d, J = 7.0 Hz, 3H), 1.50 (s, 3H), 3.15 (q, J = 7.0 Hz, 1H), 4.82 (sept, J = 7.0 Hz, 1H), 7.2−7.5 (m, 5H); ^{13}C NMR ($CDCl_3$) δ 10.4 (q), 14.5 (q), 19.3 (q), 44.0 (d), 51.6 (d), 84.6 (s), 87.2 (s), 125.9 (d), 127.9 (d), 128.2 (d), 132.4 (s), 172.6 (s), 174.1 (s). Anal. Calcd for $C_{16}H_{19}O_3N$: C, 70.31; H, 7.01; N, 5.12. Found C, 70.35; H, 6.81; N, 5.09.

X-ray crystallographic analysis of *syn*-1,7-dimethyl-3-isopropyl-5-phenyl-6-oxa-3-azabicyclo[3.1.1]heptane-2,4-dione (*syn*-2a): colorless prismatic crystals from hexane−chloroform, space group $P2_1$, a = 10.195(2) Å, b = 7.231 (4) Å, c = 10.860(2) Å, β = 112.05(1)°, V = 742.0(4) Å^3, Z = 2, ρ = 1.219 g/cm^3, μ(Cu Kα) = 6.85 cm^{-1}; R = 0.040, R_W = 0.034 for 2350 reflections.

Synthesis and the Determination of the Absolute Configuration of *syn*-1,7-Dimethyl-3-isopropyl-5-phenyl-4-oxo-6-oxa-3-azabicyclo[3.1.1]heptane-2-thione (*syn*-4a). A toluene solution of optically pure *syn*-(+)-**2a**, which was obtained by recrystallization of 95% ee of **2a**, and 0.5 equiv of Lawesson's reagent was refluxed for 2 h. Toluene was removed in *vacuo*, and the residual mixture was subjected to silica gel column chromatography using benzene as eluent. *syn*-(−)-1,7-Dimethyl-3-isopropyl-5-phenyl-4-oxo-6-oxa-3-azabicyclo[3.1.1]heptane-2-thione (*syn*-**4a**) was isolated in 90% yield and recrystallized from a chloroform−hexane mixture: slightly yellow prismatic crystals, space group $P2_1$, a = 10.976(4) Å, b = 7.241(2) Å, c = 10.407(4) Å, β = 111.25(1)°, V = 770.9(4) Å^3, Z = 2, ρ = 1.25 g/cm^3, μ(Cu Kα) = 1.54 cm^{-1}; R = 0.0665, R_W = 0.0796 for 1722 reflections. The structure was solved by the direct method and refined by the method of full-matrix least-squares. The absolute configuration was determined through refinement of Roger's parameter, whose value was 1.074, as (1*R*,5*R*,7*R*)-**4a**: mp 84−85 °C; IR (cm^{-1}, KBr) 1730; UV (nm, CH_3CN) 285 (ϵ 17 800); ^{1}H NMR ($CDCl_3$) δ 1.05 (d, J = 7.0 Hz, 3H), 1.48 (d, J = 7.0 Hz, 3H), 1.50 (d, J = 7.0 Hz, 3H), 1.68 (s, 3H), 3.11 (q, J = 7.0 Hz, 1H), 5.66 (sept, J = 7.0 Hz, 1H) , 7.2−7.5 (m, 5H); ^{13}C NMR ($CDCl_3$) δ 11.1 (q), 18.3 (q), 19.1 and 19.7 (q), 50.7 (d), 52.5 (d), 86.8 (s), 88.8 (s), 126.0 (d), 127.9 (d), 128.3 (d), 132.2 (s), 169.9 (s), 211.1 (s).

***anti*-1,7-Dimethyl-3-isopropyl-5-phenyl-6-oxa-3-azabicyclo[3.1.1]heptane-2,4-dione (*anti*-2a)** (minor isomer): ^{1}H NMR ($CDCl_3$) δ 1.19 (d, J = 7.0 Hz, 3H), 1.46 (d, J = 7.0 Hz, 3H), 1.47 (d, J = 7.0 Hz, 3H), 1.59 (s, 3H), 3.47 (q, J = 7.0 Hz, 1H), 4.82 (sept, J = 7.0 Hz, 1H), 7.2−7.5 (m, 5H); ^{13}C NMR ($CDCl_3$) 10.1 (q), 18.8 (q), 19.5 (q), 44.3 (d), 55.8 (d), 86.6 (s), 88.6 (s), 125.1 (d), 128.3 (d), 128.6 (d), 136.1 (s), 171.5 (s), 172.6 (s).

***syn*-3-Benzyl-1,7-dimethyl-5-phenyl-6-oxa-3-azabicyclo[3.1.1]heptane-2,4- dione (*syn*-2b)** (major isomer): mp 112−113 °C; IR (cm^{-1}, KBr) 1700, 1755; UV (nm, CH_3CN) 257 (ϵ 730); ^{1}H NMR ($CDCl_3$) δ 1.03 (d, J = 7.2 Hz, 3H), 1.51 (s, 3H), 3.17 (q, J = 7.2 Hz, 1H), 4.94 (s, 2H), 7.1−7.5 (m, 10H); ^{13}C NMR ($CDCl_3$) δ 10.4 (q), 14.5 (q), 42.4 (t), 51.7 (d), 84.6 (s), 87.2 (s), 125.9 (d), 127.7 (d), 127.9 (d), 128.3 (d), 128.5 (d), 128.7 (d), 132.2 (s), 136.4 (s), 172.3 (s), 173.8 (s). Anal. Calcd for $C_{20}H_{19}O_3N$: C, 74.73; H, 5.96; N, 4.36. Found: C, 74.80; H, 5.87; N, 4.37.

***anti*-3-Benzyl-1,7-dimethyl-5-phenyl-6-oxa-3-azabicyclo[3.1.1]heptane-2,4-dione (*anti*-2b)** (minor isomer): ^{1}H NMR ($CDCl_3$) δ 1.01 (d, J = 7.2 Hz, 3H), 1.59 (s, 3H,), 3.50 (q, J =7.2 Hz, 1H), 4.97 (s, 2H), 7.1−7.5 (m, 10H); ^{13}C NMR ($CDCl_3$) δ 9.86 (q), 18.7 (q), 42.2 (t), 56.3 (d), 86.6 (s), 88.6 (s), 125.0 (d), 128.4 (d), 128.8 (d), 129.2 (d), 130.5 (d), 134.5 (d), 135.8 (s), 136.3 (s), 171.3 (s), 172.3 (s).

***trans*-*N*-Tigloylbenzoylformanilide (*trans*-1c)**: ^{1}H NMR ($CDCl_3$) δ 1.70 (s, 3H), 1.75 (d, J = 7.3 Hz, 3H), 5.48 (q, J = 7.3 Hz, 1H), 7.2−7.5 (m, 8H), 7.6−7.7 (m, 2H); ^{13}C NMR ($CDCl_3$) δ 12.8 (q), 13.9 (q), 127.6 (d), 127.7 (d), 128.4 (d), 128.7 (d), 129.5 (d), 129.6 (d), 129.8 (d), 131.8 (s), 134.1 (s), 134.2 (s), 139.6 (s), 169.2 (s), 172.0 (s), 173.5 (s).

***syn*-1,7-Dimethyl-3,5-diphenyl-6-oxa-3-azabicyclo-[3.1.1]heptane-2,4-dione (*syn*-2c)** (major isomer): mp 159−160 °C; IR (cm^{-1}, KBr) 1700, 1760; UV (nm, CH_3CN) 251 (ϵ 1000); ^{1}H NMR ($CDCl_3$) δ 1.11 (d, J = 6.9 Hz, 3H), 1.58 (s, 3H), 3.43 (q, J = 6.9 Hz, 1H), 7.2−7.6 (m, 10H); ^{13}C NMR ($CDCl_3$) δ 10.5 (q), 14.6 (q), 51.5 (d), 84.9 (s), 87.4 (s), 125.1 (d), 128.1 (d), 128.3 (d), 128.4 (d), 128.8 (d), 129.2 (d), 132.5 (s), 135.7 (s), 172.0 (s), 173.5 (s). Anal. Calcd for $C_{19}H_{17}O_3N$: C, 74.20; H, 5.57; N, 4.56. Found: C, 73.98; H, 5.61; N, 4.51.

***anti*-1,7-Dimethyl-3,5-diphenyl-6-oxa-3-azabicyclo-[3.1.1]heptane-2,4-dione (*anti*-2c)** (minor isomer): ^{1}H NMR ($CDCl_3$) δ 1.37 (d, J = 6.9 Hz, 3H), 1.68 (s, 3H), 3.62 (q, J = 6.9 Hz, 1H), 7.2−7.6 (m, 10H); ^{13}C NMR ($CDCl_3$) δ 10.4 (q), 18.9 (q), 55.9 (d), 86.9 (s), 88.8 (s), 126.0 (d), 127.9 (d), 128.2 (d), 128.8 (d), 128.9 (d), 129.2 (d), 132.0 (s), 132.7 (s), 170.9 (s), 172.0 (s).

***syn*-1,7-Dimethyl-5-diphenyl-6-oxa-3-(*o*-tolyl)-3-azabicyclo[3.1.1]heptane-2,4-dione (*syn*-2d) (Major Isomer).** This material was composed of two rotamers owing to the rotation of *o*-tolyl group and the ratio was 1.9:1: mp 164−165 °C; IR (cm^{-1}, KBr) 1690, 1750; UV (nm, CH_3CN) 255 (ϵ 3000), 285 (ϵ 810); ^{1}H NMR ($CDCl_3$) δ 1.12 and 1.13 (each d, J = 6.9 Hz, total 3H), 1.58 (d, J = 1.0 Hz, 3H), 2.23 (s, 3H), 3.45 (dq, J = 1.0 and 6.9 Hz, 1H), 7.1−7.5 (m, 9H); ^{13}C NMR ($CDCl_3$) δ 10.5 (q), 14.6 (q), 17.2, 17.6 (q), 51.6 and 51.7 (each d), 85.0 and 85.1 (each s), 87.5 (s), 126.0 (d), 126.8 (d), 127.1 (d), 127.9 (d), 128.4 (d), 128.6 (d), 129.3 (d), 129.4 (d), 131.0 (d), 131.1 (d), 131.7 (s), 131.8 (s), 132.0 (s), 136.1 (s), 136.3 (s), 171.7 and 171.8 (each s), 173.3 and 173.5 (each s). Anal. Calcd for $C_{20}H_{19}O_3N$: C, 74.58; H, 5.92; N, 4.35. Found: C, 74.68; H, 5.94; N, 4.34.

***anti*-1,7-Dimethyl-5-diphenyl-3-(*o*-tolyl)-6-oxa-3-azabicyclo[3.1.1]heptane-2,4-dione (*anti*-2d) (Minor Isomer).** This material was composed of two rotamers owing to the rotation of *o*-tolyl group and the ratio was 1.9:1: ^{1}H NMR ($CDCl_3$) δ 1.40 and 1.44 (each d, J = 7.0 Hz, 3H), 1.69 (s, 3H), 2.19 and 2.31 (each s, 3H), 3.62 (q, J = 6.9 Hz, 1H), 7.1−7.5 (m, 9H); ^{13}C NMR ($CDCl_3$) δ 10.4 and 10.8 (each q), 18.6 (q), 18.9 (q), 55.8 and 56.0 (each d), 87.0 and 87.2 (each s), 88.9 (s), 125.1 (d), 126.7 (d), 128.3 (d), 128.6 (d), 128.8 (d), 129.4 (d), 131.2 (d), 131.6 (s), 135.7 (s), 136.2 (s), 170.8 (s), 171.8 (s).

***syn*-1,7-Dimethyl-5-phenyl-3-(2,6-xylyl)-6-oxa-3-azabicyclo[3.1.1]heptane-2,4-dione (*syn*-2e)** (major isomer): mp 197−198 °C; IR (cm^{-1}, KBr) 1690, 1750; UV (nm, CH_3CN) 263 (ϵ 890); ^{1}H NMR ($CDCl_3$) δ 1.13 (d, J = 6.9 Hz, 3H), 1.59 (s, 3H), 2.14 (s, 3H), 2.21 (s, 3H), 3.47 (q, J = 6.9 Hz, 1H), 7.1−7.5 (m, 8H); ^{13}C NMR ($CDCl_3$) δ 10.5 (q), 14.6 (q), 17.3, (q), 17.8 (q), 51.5 (d), 85.3 (s), 87.7 (s), 126.0 (d), 127.9 (d), 128.4 (d), 128.6 (d), 129.1 (d), 132.0 (s), 136.0 (s), 136.2 (s), 171.4 (s), 173.0 (s). Anal. Calcd for $C_{21}H_{21}O_3N$: C, 75.19; H, 6.31; N, 4.18. Found: C, 75.16; H, 6.24; N, 4.12.

***anti*-1,7-Dimethyl-5-phenyl-3-(2,6-xylyl)-6-oxa-3-azabicyclo[3.1.1]heptane-2,4-dione (*anti*-2e)** (minor isomer): ^{1}H NMR ($CDCl_3$) δ 1.46 (d, J = 7.0 Hz, 3H), 1.69 (s, 3H), 2.17, 2.29 (s, 3H), 3.66 (q, 7.0 Hz, 1H), 7.1−7.5 (m, 8H); ^{13}C NMR ($CDCl_3$) δ 10.7 (q), 17.6 (q), 19.1 (q), 19.7 (q), 55.7 (d), 87.5 (s), 89.2 (sO), 127.1 (d), 128.3 (d), 128.7 (d), 129.4 (s), 131.1(s), 131.2 (d), 135.7 (s), 136.2 (s), 171.0 (s), 173.1 (s).

3-(Benzoylmethyl)-1-isopropyl-3-methylazetidine-2,4-dione (5f): mp 79−80 °C; IR (cm^{-1}, KBr) 1680, 1720; UV (nm, CH_3CN) 244 (ϵ 12 400), 280 (ϵ 12 900); ^{1}H NMR ($CDCl_3$) δ 1.49 (d, J = 6.8 Hz, 6H), 1.49 (s, 3H), 3.38 (s, 2H), 3.98 (sept, J = 6.8 Hz, 1H), 7.2−7.7 (m, 3H), 7.8−8.0 (m, 2H); ^{13}C NMR

($CDCl_3$) δ 18.3 (q), 20.1 (q), 39.9 (t), 44.5 (d), 60.8 (s), 128.0 (d), 128.6 (d), 133.6 (d), 135.6 (s), 173.7 (s), 195.9 (s). Anal. Calcd for $C_{15}H_{17}O_3N$: C, 69.47; H, 6.61; N, 5.40. Found: C, 69.30; H, 6.60; N, 5.35.

1-(Benzoylformyl)-3,3-dimethyl-4-phenylazetidin-2-one (6g): mp 118−119 °C; IR (cm^{-1}, KBr) 1690, 1800; UV (nm, CH_3CN) 238 (ϵ 5600), 251 (ϵ 6400); ^1H NMR ($CDCl_3$) δ 0.85 (s, 3H), 1.54 (s, 3H), 5.03 (s, 1H), 7.2−7.7 (m, 8H), 7.9−8.0 (m, 2H); ^{13}C NMR ($CDCl_3$) δ 17.8 (q), 23.0 (q), 56.7 (s), 65.4 (d), 125.9 (d), 128.4 (d), 128.8 (d), 129.0 (d), 129.9 (d), 131.9 (s), 134.1 (s), 135.1 (d), 163.2 (s), 170.7 (s), 188.0 (s). Anal. Calcd for $C_{19}H_{17}O_3N$: C, 74.25; H, 5.57; N, 4.55. Found: C, 73.95; H, 5.64; N, 4.53. The enantiomeric excess was determined by ^1H-NMR spectroscopy employing 0.5 equiv of Eu(hfc)$_3$.

1-Methyl-6-oxa-3,5-diphenyl-3-azabicyclo[3.1.1]heptane-2,4-dione (2h): mp 121−122 °C; IR (cm^{-1}, KBr) 1710, 1760; UV (nm, CH_3CN) 253 (ϵ 970); ^1H NMR ($CDCl_3$) δ 1.72 (s, 3H), 3.29 and 3.41 (ABq, J = 9.7 Hz, 2H), 7.2−7.5 (m, 10H); ^{13}C NMR ($CDCl_3$) δ 19.0 (q), 46.9 (t), 81.7 (s), 83.5 (s), 124.3 (d), 127.2 (d), 127.3 (d), 127.9 (d), 128.2 (d), 131.5 (s), 134.5 (s), 170.8 (s), 171.7 (s). Anal. Calcd for $C_{18}H_{15}O_3N$: C, 73.79; H, 5.12; N, 4.78. Found: C, 73.55; H, 5.07; N, 4.66.

3-(2,6-Dichlorophenyl)-1-methyl-6-oxa-5-diphenyl-3-azabicyclo[3.1.1]-heptane-2,4-dione (2j): mp 150−151 °C; IR (cm^{-1}, KBr) 1720, 1770; UV (nm, CH_3CN) 263 (ϵ 770), 278 (ϵ 520); ^1H NMR ($CDCl_3$) δ 1.76 (s, 3H), 3.46 (br, 2H), 7.3−7.5 (m, 8H); ^{13}C NMR ($CDCl_3$) δ 19.8 (q), 47.7 (t), 83.0 (s), 84.8 (s), 125.4 (d), 128.4 (d), 128.8 (d), 129.0 (d), 131.0 (d), 135.0 (s), 135.2 (s), 135.3 (s), 170.0 (s), 171.0 (s). Anal. Calcd for $C_{18}H_{13}O_3NCl_2$: C, 59.83; H, 3.63; N, 3.88. Found: C, 59.75; H, 3.58; N, 3.94.

JO9704974